



Zachary P. Klicka and Badr Ebraheem*

and the corresponding eigenvalues are $\lambda_1 = 2$, $\lambda_2 = 4, 10$, and $\lambda_3 = 2$,
 $\lambda_4 = 14$.

A page of musical notation for a string quartet, featuring four staves with various notes and rests. The page includes measure numbers 3 and 12, and a page number 44 at the bottom center.

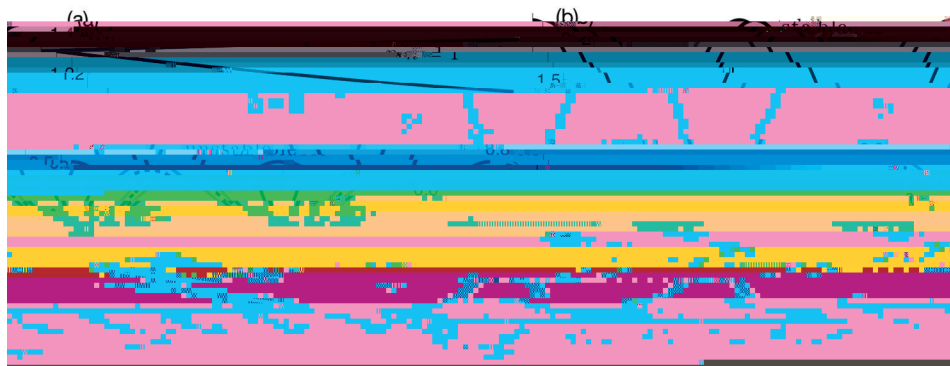


FIG. 1. *Input-locked bumps in the deterministic neural field (1.1) with input (2.3). (a) The bump half-width δ for a unimodal ($\sigma = 1$) and bimodal ($\sigma = 2$) input calculated using (2.7) and*

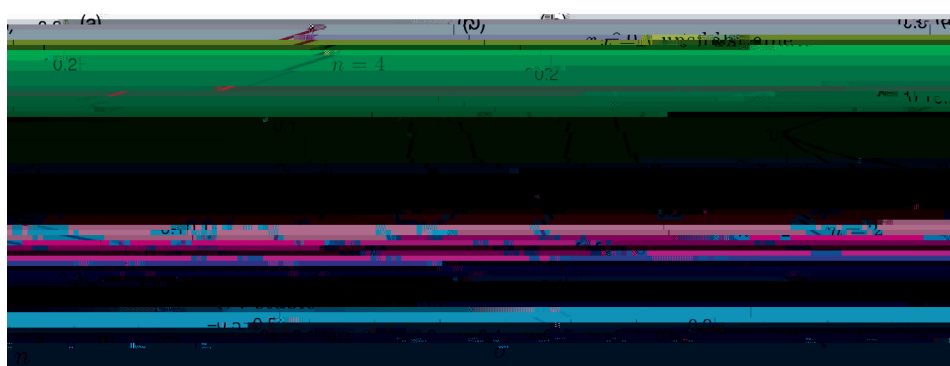
10, 33, (1.2). (2.10) (2.10)

$$(2.10) \quad o^{-} = \frac{0}{()}$$

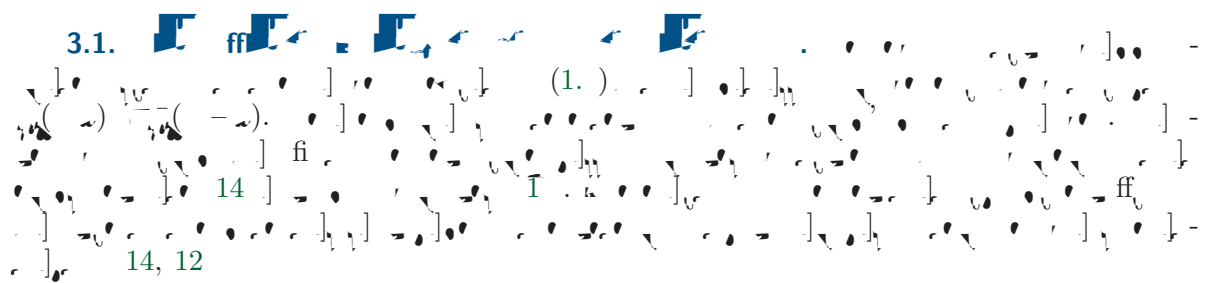
(.14). (1.). (2.10) (2.10)

$$o^{-} = 0 ()$$





4. *Eigenvalue λ_0*



(3.) $\Delta(\omega) = \frac{\int_{\omega}^{\infty} (\omega')^{-1/2} \frac{(\omega')^{-1/2}}{\int_{\omega}^{\infty} (\omega')'(\omega')} d\omega'}{\int_{\omega}^{\infty} (\omega')^{-1/2} d\omega'}$

$\Delta(\omega)^2 = \frac{\int_{\omega}^{\infty} \int_{\omega}^{\infty} (\omega')(\omega')^{-1/2} (\omega')^{-1/2} (\omega - \omega') d\omega' d\omega}{\left[\int_{\omega}^{\infty} (\omega')'(\omega') d\omega' \right]^2}$

(3.) $\Delta(\omega)^2 = \frac{\int_{\omega}^{\infty} \int_{\omega}^{\infty} (\omega')(\omega')^{-1/2} (\omega - \omega') d\omega' d\omega}{\left[\int_{\omega}^{\infty} (\omega')'(\omega') d\omega' \right]^2}$

3.3.



(1.3

ff } eff (1.) (1.3)

4.

A musical score for "The Star-Spangled Banner" in F major. The score consists of two staves. The top staff begins with a treble clef, a key signature of one sharp, and a common time signature. The bottom staff begins with a bass clef and a common time signature. The lyrics are written in blue ink, with some words in green ink, such as "Star-Spangled" and "Banner". The music includes various dynamics like forte, piano, and sforzando, and features a mix of eighth and sixteenth note patterns.

4.1.

A handwritten musical score for piano, page 41, featuring ten measures of music. The score includes two systems of staves, with dynamics such as forte (f), piano (p), and sforzando (sf). Measure 1 starts with a forte dynamic. Measures 2-3 show a transition with eighth-note patterns. Measures 4-5 continue with eighth-note patterns and dynamics. Measures 6-7 show a continuation of the eighth-note patterns. Measures 8-9 show a continuation of the eighth-note patterns. Measure 10 concludes with a forte dynamic.

$$(4.1) \quad (\quad - \alpha) \quad \vdash , \quad (\quad - \alpha)$$

$$[v] = \text{ff}_v \quad \text{ffi} \quad (3.1) \quad v$$

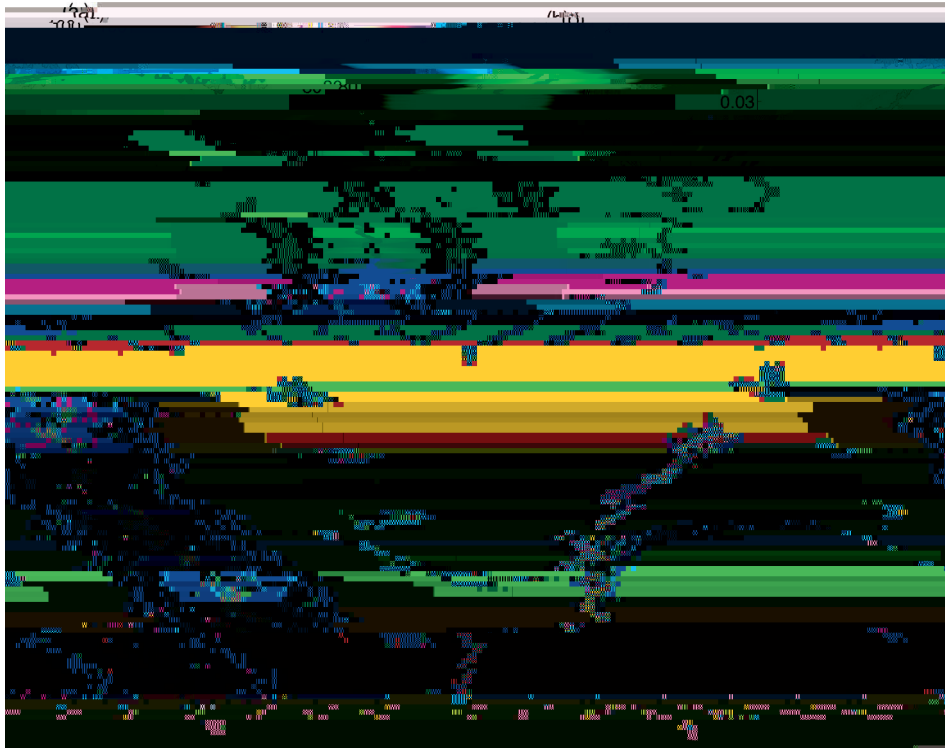
$$(4.2) \quad \left(\int_{\Gamma} \left[\frac{\partial}{\partial n} \left(\int_{\Gamma} u^2 \right)^{1/2} \right]^2 + \left(\int_{\Gamma} u' \left(\int_{\Gamma} u^2 \right)^{1/2} \right)^2 \right]^{1/2}$$

find the value of $\left(\frac{1}{2}\right)$, $(\frac{1}{3})$, $(\frac{1}{4})$.



 . Bumps pinned by stationary inputs (2.3) in the stochastic neural field (1.7)

4. **E**. fi
 (1.), (1.2) () (4.3). (4.1).



E. Pinning of bumps in the network (1.7) with synaptic weight (1.4) for low frequency synaptic heterogeneity. (a) Numerical simulation of (1.7) using synaptic weight (1.4) for $\gamma = 2$, $\sigma = 0.1$, and $\varepsilon = 0.01$ shows that the bump remains pinned to the stable attractor at $\theta = 0$. (b) The variance of the bump's position plotted against time computed numerically (red dashed) across 1000 realizations saturates after a moderate amount of time when $\gamma = 2$, as predicted by the Ornstein–Uhlenbeck approximation (3.20) (blue solid). (c) Numerical simulation for $\gamma = 3$, $\sigma = 0.1$, and $\varepsilon = 0.01$ shows that the bump remains pinned to the stable location at $\theta = 0$. (d) The variance of the bump's position plotted against time computed numerically ($r5.3(ti)-10.5F9(t)3.nwh$)

$$(1.14) \quad \int_0^1 \phi'(x) \psi''(x) dx = - \int_0^1 \phi(x) \psi'''(x) dx.$$

DOI 10.1137/10081122X
© 2012 Society for Industrial and Applied Mathematics

Copyright © by SIAM. Unauthorized reproduction of this article is prohibited.

-
- [5] R. Ben-Yishai, D. Hansel , and H. Sompolinsky, *Traveling waves and the processing of weakly tuned inputs in a cortical network module*, J. Comput. Neurosci., 4 (1997), pp. 57–77.
 - [6] C. A. Brackley and M. S. Turner, *Random fluctuations of the firing rate function in a continuum neural field model*, Phys. Rev. E, 75 (2007), 041913.
 - [7] P. C. Bressloff, *Traveling fronts and wave propagation failure in an inhomogeneous neural network*, Phys. D, 155 (2001), pp. 83–100.
 - [8] P. C. Bressloff, *Stochastic neural field theory and the system-size expansion*, SIAM J. Appl. Math., 70 (2009), pp. 1488–1521.
 - [9] P. C. Bressloff, *Spatiotemporal dynamics of continuum neural fields*

-
- [31] O. Faugeras, R. Veltz, and F. Grimbert, *Persistent neural states: Stationary localized activity patterns in the nonlinear continuous -population, -dimensional neural networks*, Neural Comput., 21 (2009), pp. 147–187.
 - [32] R. Festa and E. G. Dagliano, *Diffusion coefficient for a Brownian particle in a periodic field of force: I. Large friction limit*, Phys. A, 90 (1978), pp. 229–244.
 - [33] S. E. Folias and P. C. Bressloff, *Breathing pulses in an excitatory neural network*, SIAM J. Appl. Dyn. Syst., 3 (2004), pp. 378–407.
 - [34] S. E. Folias and P. C. Bressloff, *Breathers in two-dimensional neural media*, Phys. Rev. Lett., 95 (2005), 208107.
 - [35] S. Funahashi, C. J. Bruce, and P. S. Goldman-Rakic, *Mnemonic coding of visual space in the monkey's dorsolateral prefrontal cortex*, J. Neurophysiol., 61 (1989), pp. 331–349.
 - [36] J. M. Fuster, *Unit activity in prefrontal cortex during delayed-response performance: Neuronal correlates of transient memory*, J. Neurophysiol., 36 (1973), pp. 61–78.
 - [37] C. W. Gardiner, *Handbook of Stochastic Methods for Physics, Chemistry, and the Natural Sciences*, 3rd ed., Springer-Verlag, Berlin, 2004.
 - [38] P. S. Goldman-Rakic, *Cellular basis of working memory*, Neuron, 14 (1995), pp. 477–485.
 - [39]

[57] J. B. Levitt, D. A. Lewis, T. Yoshioka, and J. S. Lund, *Topography of pyramidal neuron intrinsic*